Nanomedicine: Nanotechnology, Biology, and Medicine
24 (2020) 102120

nanomedjournal.com

# A versatile theranostic nanodevice based on an orthogonal bioconjugation strategy for efficient targeted treatment and monitoring of triple negative breast cancer

María Victoria Cano-Cortes, PhD[a,b,d,1], Saúl Abenhamar Navarro-Marchal, MSc[c,e,f,1], María Paz Ruiz-Blas, Techn[a,b,d], Juan José Diaz-Mochon, PhD[a,b,d], Juan Antonio Marchal, Prof., PhD, MD[c,d,f,*], Rosario M. Sanchez-Martin, PhD[a,b,d,**]

[a]*GENYO, Centre for Genomics and Oncological Research, Pfizer/University of Granada/Andalusian Regional Government, PTS Granada, Granada, Spain*
[b]*Department of Medicinal & Organic Chemistry and Excellence Research Unit of "Chemistry applied to Biomedicine and the Environment," Faculty of Pharmacy, University of Granada, Campus de Cartuja s/n, Granada, Spain*
[c]*Biopathology and Regenerative Medicine Institute (IBIMER), Centre for Biomedical Research (CIBM), University of Granada, Granada, Spain*
[d]*Instituto de Investigación Biosanitaria de Granada (ibs.GRANADA), Universidad de Granada, Granada, Spain*
[e]*Department of Applied Physics, Faculty of Sciences, University of Granada, Granada, Spain*
[f]*Department of Human Anatomy and Embryology and Excellence Research Unit "Modeling Nature" (MNat), Faculty of Medicine, University of Granada, Granada, Spain*

Revised 10 October 2019

## Abstract

A novel chemical-based orthogonal bioconjugation strategy to produce tri-functionalized nanoparticles (NPs) an chemotherapy drug, doxorubicin (DOX), a near-infrared cyanine dye (Cy7) and CRGDK homing peptide, a peptide specifically binds to neuropilin-1 (Nrp-1) overexpressed on triple negative breast cancer (TNBC) cells, has been validated. These theranostic NPs have been evaluated *in vitro* and *in vivo* using an orthotopic xenotransplant mouse model using TNBC cells. *In vitro* assays show that theranostic NPs improve the therapeutic index in comparison with free DOX. Remarkably, *in vivo* studies showed preferred location of theranostic NPs in the tumor area reducing the volume at the same level than free DOX while presenting lower side effects. This multifunctionalized theranostic nanodevice based on orthogonal conjugation strategies could be a good candidate for the treatment and monitoring of Nrp-1 overexpressing tumors. Moreover, this versatile nanodevice can be easily adapted to treat and monitor different cancer types by adapting the conjugation strategy.

*Key words:* Polymeric nanoparticles; Orthogonal chemistry; Covalent conjugation; Doxorubicin; CRGDK targeting; Multifunctional theranostic nanodevice

*Abbreviations:* AFM, atomic force microscopy; ANOVA, analysis of variance; BCA, bicinchoninic acid; Cy7, cyanine7; CRGDK, Cys-Arg-Gly-Asp-Lys; Dde, ethyl 1- (4,4-dimethyl-2, 6-dioxocyclohexylidene; DIC, N,N′-diisopropylcarbodiimide; DIPEA, N,N-diisopropylethylamine; DLS, dynamic light scattering; DMEM, Dulbecco's modified Eagle's medium; DMF, dimethylformamide; DOX, doxorubicin; FBS, fetal bovine serum; Fmoc, fluorenylmethyloxycarbony; HPLC, high performance liquid chromatography; IC, inhibitory concentration; IVIS, *in vivo* fluorescence analysis; NPs, nanoparticles; PBS, phosphate-buffered saline; PEG, polyethylene glycol; PLGA, poly (lactic-co-glycolic acid); ROS, reactive oxygen species; TNBC, triple negative breast cancer; TEM, transmission electron microscopy

E-mail address: support@elsevier.com (Global Customer Service).

Acknowledgements: This work was supported by grants from the Ministry of Economy and Competitiveness (MINECO, National Programme for Research Aimed at the Challenges of Society, project reference BIO2016-80519-R&FEDER funds, grant number MAT2015-62644.C2.2.R), by Ministerio de Ciencia, Innovación y Universidades grant number RTI2018-101309-B-C2 (FEDER Funds), the Health Institute Carlos III (ISCIII) (Projects of technological development in health - ref DTS18/00121) and the Chair "Doctors Galera-Requena in cancer stem cell research". This research was additionally supported by the University of Granada – PLAN OF RESEARCH AND TRANSFER 2016 –PSETC- PSE/16/003). The authors thank the Research Results Transfer Office (OTRI) of the University of Granada for their support for the technological development of this project. S.A.N-M. acknowledges the MINECO for providing a PhD fellowship (FPI) through the project MAT2015-62644.C2.2.R.

Conflicts of interest: There are no conflicts to declare.

*Corresponding author at: Biopathology and Regenerative Medicine Institute (IBIMER), Centre for Biomedical Research (CIBM), University of Granada, Granada, 18100, Spain.

**Corresponding author at: GENYO, Centre for Genomics and Oncological Research, Pfizer/University of Granada/Andalusian Regional Government, PTS Granada, 18016 Granada, Spain.

*E-mail addresses:* jmarchal@ugr.es, (J.A. Marchal), rosario.sanchez@genyo.es. (R.M. Sanchez-Martin).

[1] Both authors contributed equally.

https://doi.org/10.1016/j.nano.2019.102120
1549-9634/

Theranostic nanodevices are capable of both delivering therapy and tracking disease through imaging. To produce these nanodevices combining cancer therapy and disease monitoring, synthetic methods for the effective multifunctionalization of NPs with a therapeutic cargo together with a ligand for selective delivery and a fluorophore to allow efficient tracking using fluorescence based imaging detection have to be developed, being this issue one of the challenges to produce theranostic nanodevices.[1,2] Most common approaches used for preparing theranostic NPs comprise drugs and trackers to be heterogeneously encapsulated in the core of the NP while ligands for targeted delivery are conjugated to the surface of the NP.[3,4] However, the versatility of these systems can be compromised due to incompatibilities between the conjugation chemistries and the encapsulation protocols. Consequently, there is still a gap to improve the loading efficiency of each component of the theranostic nanodevices. Over the last decade, our group has developed several strategies for preparing functionalized polymeric cross-linked polystyrene NPs, which are then covalently conjugated to cargoes of different nature (fluorophores, small drugs, proteins, nucleic acids and their mimics).[5,6] The main benefits of using polystyrene NPs are their robustness and stability in the biological environment, their lack of cellular toxicity during long term incubations[7] and their compatibility with standard multistep chemistries, allowing different orthogonal conjugation strategies. All of these features allow their easy entry in a broad range of cell types.[5,6,8–10] Remarkably, gene-expression profiling studies showed that these NPs did not induce any significant alteration in nanofected cell transcriptomes.[11] Proteomic studies showed that no key regulators of cell cycle were affected by the internalization of these NPs (their intracellular localization has been proven).[12] Recently, the development of an efficient nanotechnology fluorescence-based method to track cell proliferation to avoid the limitations of current cell-labelling dyes has been reported.[13] Additionally, the design of a straightforward strategy to conjugate drugs *via* click chemistry to NPs as a novel tool to study target engagement and/or identification inside living cells was recently presented.[14] All of these properties make these polymeric NPs promising candidates for cancer theranostic applications.

Herein, we report a chemical-based orthogonal strategy for NPs multifunctionalization that opens the door for the design of a versatile nanodevice that allows the covalent conjugation of a therapeutic cargo, a ligand and a tracker in a controlled manner. This strategy allows tuning the ratio between the amount of each one of the components. This highly controlled strategy increases the possibilities of developing more effective and reproducible nanodevices for controlled released at the desired location, with minimal off-target release that may compromise healthy tissue, together with monitoring in real time. A significant advantage in covalently linking therapeutic cargoes to a vehicle system over conventional encapsulation approaches is the ability to have better control over loading and drug release. In addition, the covalent binding of the drug to the nanosystem tackle another problem faced by current treatments, low water solubility and leaking from the nanoencapsulation. The presence of a fluorophore tracker on the theranostic nanoparticle allows monitoring tumor location, disease evolution and treatment efficiency. The tri-functionalized NPs carrying doxorubicin (DOX), near-infrared cyanine dye (Cy7) and a homing peptide (CRGDK), which can actively recognize the neuropilin-1 (Nrp-1) receptor (overexpressed in triple negative breast cancer),[15] were evaluated *in vitro* using triple negative breast cancer cell line (TNBC, MDA-MB-231) and *in vivo* using an orthotopic breast cancer xenotransplant mouse model.

## Methods

### *Preparation of theranostic nanoparticles (HP-Cy7-DOX-NPs (14))*

All solvents and chemicals were purchased from Sigma-Aldrich. Double PEGylated and bifunctionalized NPs (Fmoc-Dde-NPs**, 6**) were obtained by using protocols previously described[16] (see S.I.). Next, DOX-NPs (**9**) were obtained by carboxy functionalization and hydrazine treatment followed by DOX conjugation (see S.I.) Then trifunctionalized NPs were generated by treatment with Fmoc-lysine-Dde(OH) (15 equiv), Fmoc deprotection and fluorophore conjugation (see S.I.). Finally, COOH-Cy7-DOX-NPs (**13**) were activated with oxyma (15 equiv) and DIC (15 equiv) and were functionalized with a solution of CRGDK homing peptide (see S.I.) in DMF and DIPEA at 25 °C for 15 hours to obtain (HP-Cy7-DOX-NPs (**14**)).

### *Characterization of theranostic nanoparticles*

Particle mean size, size distribution and zeta potential of HP-Cy7-DOX-NPs (**14**) were determined by dynamic light scattering (DLS) and were measured on a Zetasizer Nano ZS ZEN 3500 (Malvern Panalytical) (see S.I.). The shape and morphology of the NPs were observed using transmission electron microscopy (TEM) and atomic force microscopy (AFM) (Park Systems) using Xei data acquisition software. The conjugation of the Cy7 fluorophore to the NPs was checked by flow cytometry using FACSCanto II (Becton Dickinson & Co.) and Flowjo® 10 software for data analysis.

### *Doxorubicin release profile*

Analysis of drug release efficiency was carried out using high performance liquid chromatography (HPLC) (Agilent 1200 series HPLC system) (see S.I.).

### *Cell cultures*

Cell line was provided by the cell bank of the CIC of the University of Granada. For this study, we used the triple negative human breast cancer cell line MDA-MB-231. This cell line was cultured in DMEM base medium (Gibco) supplemented with 10% (v/v) fetal bovine serum, 1% L-glutamine and 1% penicillin/streptomycin in a humidified incubator at 5% CO2 and 37 °C.

### *Nanofection of MDA-MB-231 cell line*

MDA-MB-231 cells were incubated with different ratio cell/NPs of HP-Cy7-DOX-NPs (**14**) at the established incubation times. Aminomethyl NPs calls Naked NPs (**1**) and DOX-Cy7-NPs (**11**) were used as control (at the specific ratio cell/NPs), and

cells without NPs treatment. After that, it was detached and washed with PBS 1×. Then, samples were fixed in 2% paraformaldehyde and analyzed *via* flow cytometry and confocal microscopy (see S.I).

*Cell viability*

The cellular cytotoxicity of NPs was evaluated using resarzurin assay (see SI).

*Orthotopic xenotransplant mouse model*

All *in vivo* experiments were performed in female NOD scid gamma mice (NSG, NOD.Cg-Prkdcscid Il2rgtm1Wjl/SzJ) purchased from Charles River (Barcelona, Spain). Animal welfare and experimental procedures were carried out in accordance with institutional (Research Ethics Committee of the University of Granada, Spain) and international standards (European Communities Council directive 86/609). Orthotopic xenotransplant model was done as previously reported.[17] (see SI).

*Statistical analysis*

The data are presented as the mean ± the standard deviation in the error bars. The sample size (n) indicates the experimental repeats of a single representative experiment, with 3 being unless otherwise specified. The results of the experiments were validated by independent repetitions. Graphs and statistical difference data were made with GraphPad Prism 6.0 (Graphpad Software Inc.). Statistical significance was determined using Student's t-test in paired groups of samples with known median and 2-way repeated measures ANOVA followed by Bonferroni test compared to more than two groups of samples. A p-value of $\leq 0.05$ was considered significant.

## Results

*Preparation and characterization of NPs (HP-Cy7-DOX-NPs (14)) as theranostic probes*

A chemical strategy was developed to prepare multifunctionalized polymeric NPs. A monodisperse population of aminomethyl polystyrene cross-linked NPs were prepared by dispersion polymerization using a previously reported protocol.[17] Size distribution was determined by DLS showing homogeneous size and low polydispersity (460 nm with a PDI of 0.042). Zeta potential value was 81.2 ± 0.1 mV. The concentration of NPs ($4 \times 10^6$ NP/μL ± $1.44 \times 10^{-5}$) was calculated according to the method developed by our research group (see S.I.).[18] After coupling reactions, their efficiencies were monitored by Kaiser colorimetric test.[19] Loading of starting aminomethyl NPs (**1**) (54 μmol/g) was calculated using the Fmoc test[20] following coupling of Fmoc-Gly-OH amino acid to these NPs (**1**).

To achieve the efficient covalent functionalization of three different chemical structures to NPs an orthogonal strategy had to be designed. Our strategy is based on the fully orthogonality between Dde and Fmoc protecting groups.[21,22]

Aminomethyl NPs (**1**) were thus trifunctionalized as describe in Figure 1. Firstly, NPs were double PEGylated[23] Subsequently, these NPs were bifunctionalized as previously described then double PEGylation was again carried out to achieve Fmoc-Dde-NPs (**6**) (see S.I.).[21] Then, drug conjugation was carried out to hydrazine functionalized nanoparticle through a pH labile hydrazone bond obtaining the conjugates DOX-NP (**9**). Then, a second Fmoc-Lys(Dde)–OH unit was coupled to the DOX-NPs (**9**) to yield trifunctional NPs (**10**). Then, a near infrared cyanine fluorophore (Cy7, $\lambda_{exc}$ = 750 nm, $\lambda_{em}$ = 773 nm) was conjugated using its NHS derivative to give rise to the COOH-Cy7-DOX-NPs (**13**), which can be tracked *in vivo*. Finally, CRGDK peptide was coupled to NPs *via* chemoselective conjugation**.** In order to do so, the N-terminal end of the CRGDK peptide was modified with an aminooxy acetyl group (see S.I.), which allows immobilization of the peptide to the COOH-Cy7-DOX-NPs (**13**), through the formation of an *N*-alkoxyamide bond following activation of the carboxylic group of the NPs with oxyma/DIC to obtain the final HP-Cy7-DOX-NPs (**14**). Control NPs without conjugation of CRGDK for targeted delivery were prepared (Cy7-DOX-NPs (**11**) (see SI).

Size distributions of the NPs were controlled after each key conjugation step by DLS (Figure 2, *A*, Figure S10). It can be observed that this multifunctionalization strategy did not affect the NP size. These results confirm that trifunctionalized NPs were stable and aggregation did not occur. These DLS size results were corroborated by TEM analysis (Figure 2, *B*) and by AFM (Figure 2, *C*).

Figure 2, *A* shows the zeta potential values in aqueous environments at pH 7.4 which shown negative values of HP-Cy7-DOX-NP (**14**). These results also confirm the ability of zeta potential measurements to monitor the success of the chemical modifications of NPs.[24]

In order to measure the labelling level of the theranostic nanoparticles, HP-Cy7-DOX-NPs (**14**) was analyzed by flow cytometry, confocal microscopy (Figure 2 **D-E**) and UV spectroscopy (Figure S1). The conjugation efficiency was 74.1%. Taking into account the number of NPs used in this assay ($5.2 \times 10^7$ NPs/μL), we can estimate a final concentration of $9.5 \times 10^{-8}$ nmol of Cy7/NP that correspond to $5.7 \times 10^7$ molecules of Cy7/NP.

The efficiency of conjugation of the CRGDK homing peptide to the theranostic NPs (HP-Cy7-DOX-NPs (**14**)) was determined by measuring the initial and final peptide concentration in the reaction vessel by BCA test.[25] The absorbance values obtained at 562 nm were translated into concentration using a standard calibration curve (Figure S2). The obtained results show a conjugation efficiency of 80.7%. Taking into account the number of NPs used ($1.83 \times 10^8$ NPs/μL), we can estimate a final concentration of $8 \times 10^{-9}$ nmol of CRGDK /NP that correspond to a density of $5.23 \times 10^7$ CRGDK molecules / NP.

In order to evaluate the conjugation efficiency of DOX to theranostic NPs (HP-Cy7-DOX-NPs (**14**)) the unconjugated drug which remains in the supernatant of the reaction was measured by UV spectroscopy. A calibration curve, with lineal ratio between the optic density of DOX and its concentration, was previously performed (Figure S3). The conjugation efficiency was calculated to be 72%. As the number of NPs used in this assay were $5.2 \times 10^7$ NPs/μL, we can estimate a final concentration of $1.4 \times 10^{-8}$ nmol DOX per NP that correspond to $8.4 \times 10^7$ molecules of drug per NP. It is remarkable the fact that the final amount of each component is in the same range ($10^7$ molecules per nanoparticle) to achieve each of the specific functions of this nanosystem.

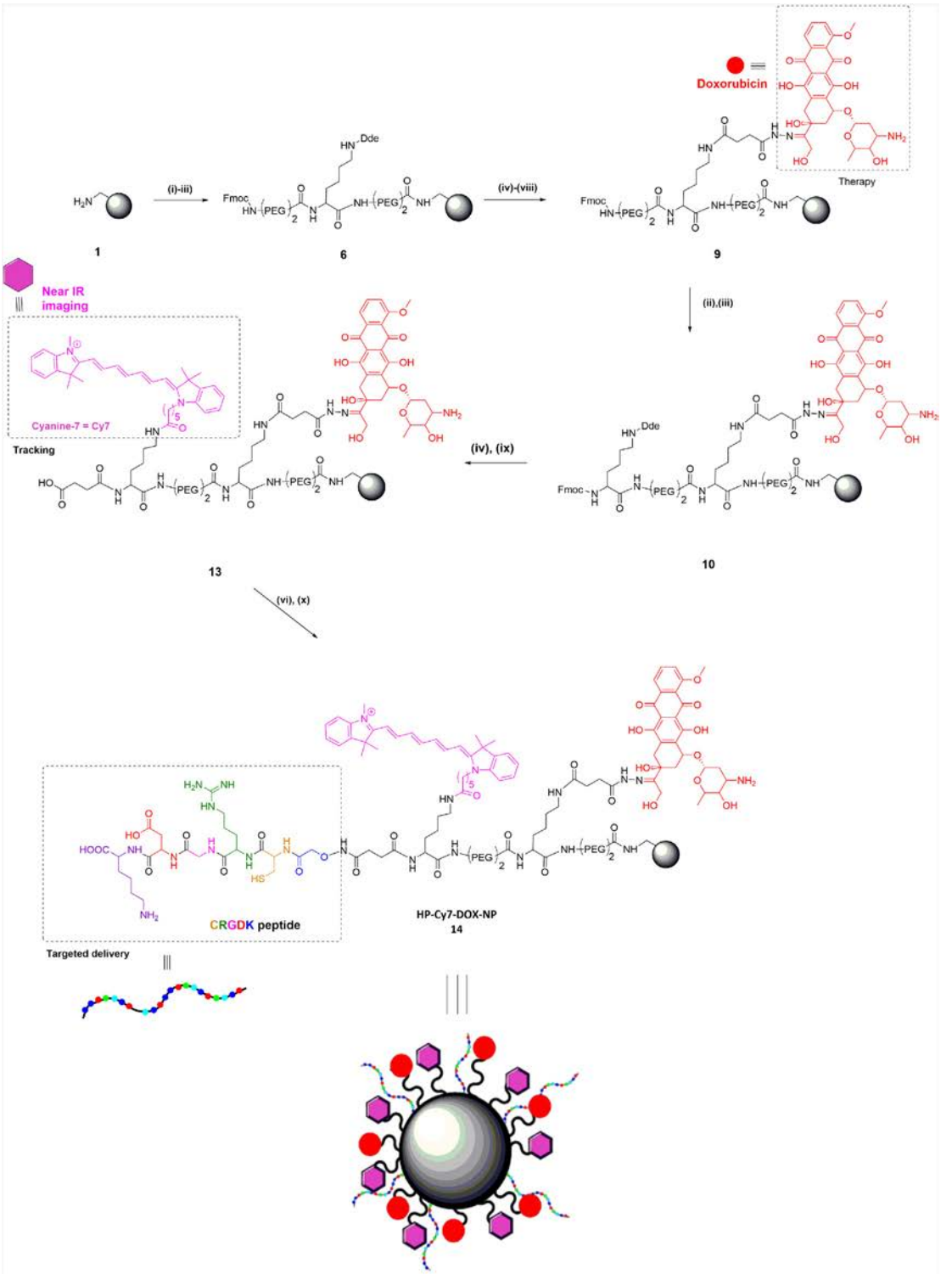


Reagents and conditions (i) Fmoc-PEG-OH (15 equiv), Oxyma (15 equiv), DIC (15 equiv), DMF. 2 h, 60 °C; (ii) 20% piperidine, DMF, 3 x 20 min; (iii) Fmoc-Lys (Dde) -OH, oxyma (15 equiv), oxyma (15 equiv), DIC (15 equiv), DMF. 2 h, 60 °C; (iv) Hydroxylamine HCl, Imidazole, NMP, 2x 1 h, 25 °C; (v) Succinic anhydride (15 equiv), DIPEA (15 equiv), 2 h., 60 ºC; (vi) Activation COOH group with oxyma (15 equiv), DIC (15 equiv), 2 h, 25 ºC; (vii) hydrazine, 55% v/v (15 equiv), 15 h, 25 °C; (viii) DOX, PBS pH 6, 15 h, 25 °C; (ix) Cy7-NHS (1 equiv), DIPEA (0.1 equiv), 15 h, 25 °C; (x) CRGDK (7 equiv), DIPEA (0.1 equiv), 15 h, 25 °C.

Figure 1. General scheme of synthesis of theranostic nanoparticles (HP-Cy7-DOX-NPs (**14**)).

A)

| NPs | Diameter Mean (nm) | PDI | Zeta potencial (mV) |
|---|---|---|---|
| Amino methyl NP (1) | 460 ± 0.4 | 0.042 | 81.2 ± 0.2 |
| Fmoc-Dde-NP(6) | 462.3 ± 1.0 | 0.1 | -37,8 ± 0.62 |
| Hydrazine NP (8) | 463.3 ± 1.6 | 0.085 | 31.4 ± 0.3 |
| DOX-Cy7-NP (11) | 466 ± 0.7 | 0.013 | -17 ± 1.4 |
| DOX-HP-Cy7-NP (14) | 462.8 ± 1.2 | 0.015 | -18.6 ± 0.6 |

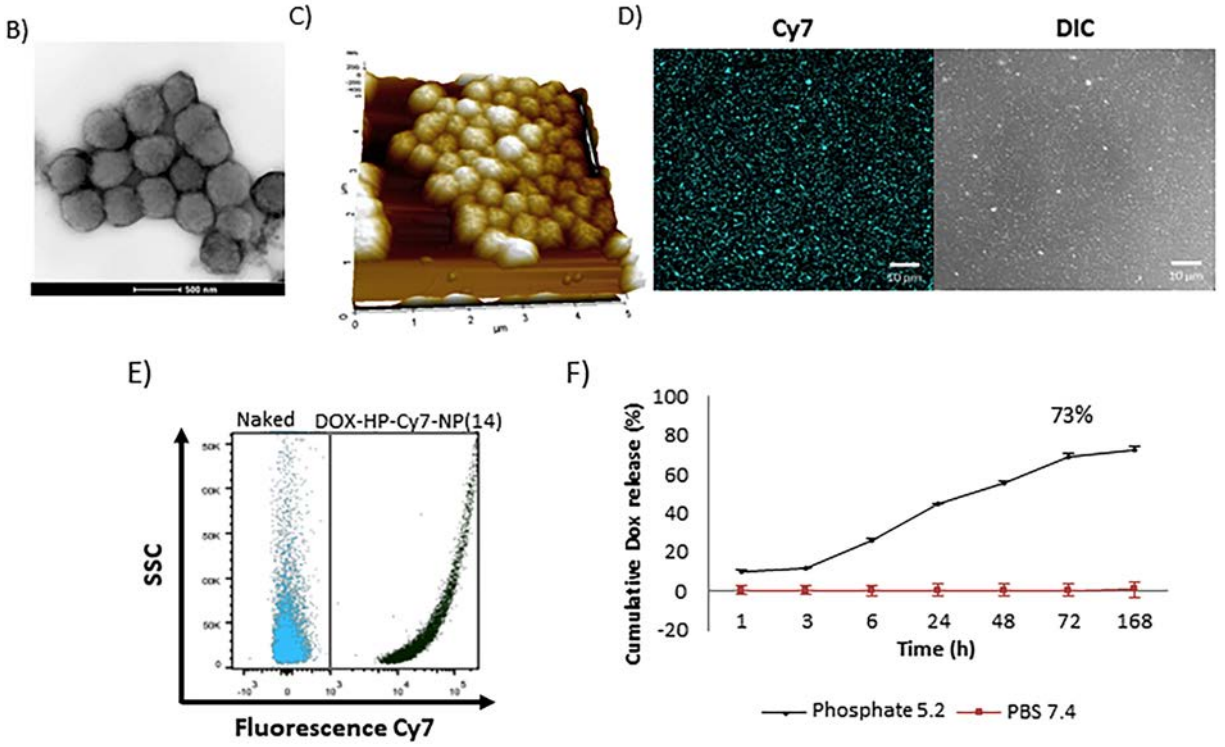


Figure 2. Physicochemical characterization of theranostic NPs (HP-Cy7-DOX-NPs (14)). A) Table with particle size distribution (nm) and zeta potential; B) TEM; C) AFM; D) Confocal microscopy, Scale bar, 10 μm; E) Representative overlay dot plot obtained after flow cytometry analysis of naked NPs (**1**) (blue) and HP-Cy7-DOX-NPs (**14**) (green); F) Cumulative DOX release. The results have been expressed with the values of the mean ± SEM.

The efficiency of DOX release from HP-Cy7-DOX-NPs (**14**) was determined by performing UV spectroscopy of the buffers in which HP-Cy7-DOX-NPs (**14**) were incubated and using a HPLC system (Figure S4 and Figure S11). HP-Cy7-DOX-NPs (**14**) where incubated at pH 5.2 (phosphate buffer) at which pH sensitive hydrazone bonds are reversible cleaved**.** A significant drug release of 44% ± 0.1 after 24 hours of incubation at pH 5.2 was observed. Then, a sustained release occurs up to 168 hours incubation, achieving a maximum release value of 73%. In contrast, there is no significant loss of DOX conjugated to NPs when incubation is carried out in 7.4 pH PBS (Figure 2, *F*). Consequently, an efficient and selective drug release at acidic pH has been achieved.

*Cellular uptake of theranostic nanoparticles is due to a receptor-mediated binding mechanism*

To initially investigate the effect of conjugation of the different bioactive cargoes on cellular uptake, these theranostic NPs (HP-Cy7-DOX-NPs (**14**)) were evaluated using a triple negative breast cancer cells (TNBC, MDA-MB-231) that are characterized by rapid grow rate and to be remarkable aggressive and metastatic. These cells are thus a perfect candidate to evaluate these theranostic nanodevices for two reasons: (i) they overexpress Nrp-1, which is the targets of the CRGDK homing peptide[26] and, (ii) DOX is a drug of choice for the treatment of triple negative breast cancer.[27]

Several assays were carried out to determine the number of HP-Cy7-DOX-NPs (**14**) required to achieve an efficient uptake by flow cytometry analysis. As a first approach, a range of concentrations of NPs from 50 to 20,000 NPs/cells were evaluated following 24 h of incubation. Then, cells were detached, fixed and analyzed by flow cytometry. Untreated cells and cell treated with Naked NPs (**1**) and NPs without CRGDK, Cy7-DOX-NP (**11**) were used as controls. Figure 3 shows results obtained by flow cytometry. It can be observed that uptake of theranostic NPs (HP-Cy7-DOX-NPs (**14**)) is very efficient and concentration dependent (Figure 3, *A* and *B*). Efficient uptake was corroborated by confocal microscopy (Figure 3, *F*). It is interesting to highlight the lower internalization of HP-Cy7-DOX-NPs (**14**) compared to Cy7-DOX-NP (**11**). Additionally,

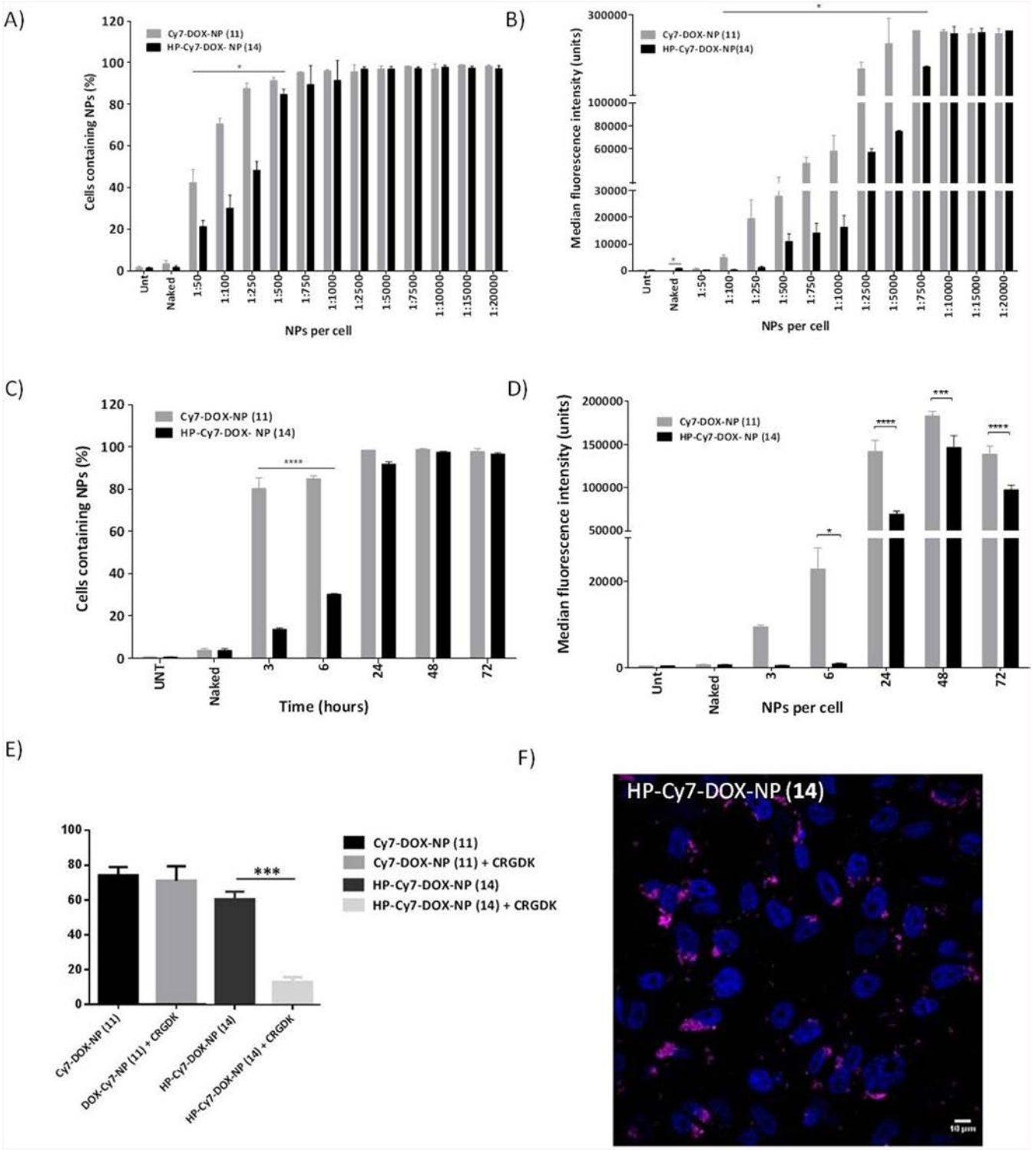


Figure 3. Evaluation of cellular uptake of theranostic NPs (HP-Cy7-DOX-NPs (**14**)) and control NPs without homing peptide (Cy7-DOX-NPs (**11**)) in the MDA MB 231 cell line. Analysis of cellular uptake *versus* NPs concentration at 24 hours (A) % cells containing NPs and (B)) B) Analysis of cellular uptake *versus* time by ΔMFI C) Bar representation to compare nanofection cellular between NPs **14** and **11** at different times; D) Bar representation to compare ΔMFI between NPs **14** and **11** at different times. Statistical significance was determined by 2-way repeated measures ANOVA followed by Bonferroni test, n = 6, (*$P < 0.05$, ****$P < 0.0001$. The results have been expressed with the values of the mean ± SEM; E) Competitive binding assay with CRGDK homing peptide; F) Confocal microscopy of the cellular uptake behavior of theranostic NPs (HP-Cy7-DOX-NPs (**14**)).

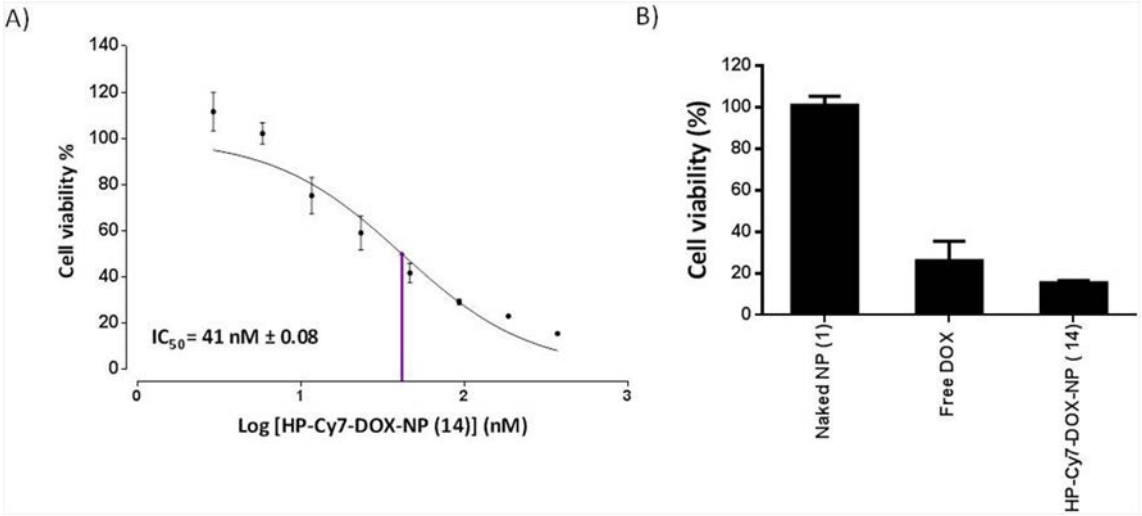


Figure 4. Evaluation of theranostic NPs (HP-Cy7-DOX-NPs (**14**)) as targeted drug delivery by the CRGDK homing peptide in the MDA MB 231 cell line. A) Half maximal inhibitory concentration ($IC_{50}$) (nM); B) Cytotoxic effect on cell viability when added 500 nM of theranostic NPs (**14**)) compared to control NPs ((**1**)) and free DOX (500 nM). The results have been expressed with the values of the mean ± SEM.

when the mean fluorescence intensity is analyzed (Figure 3, *B*), we can observe that nanofection keep increasing until cell saturation is reached (when 10,000 NPs are added per cell).

To evaluate the influence of the incubation time on the internalization, HP-Cy7-DOX-NPs (**14**) were compared with Cy7-DOX-NPs (**11**) (without ligand) for selective release during a period of 72 hours, at different time intervals (3, 6, 24, 48 and 72 hours), using 5000 NPs/cell. As we can see in Figure 3, *C* and *D*, after 3 hours of incubation, maximum nanofection was achieved, with a clear difference between both types of NPs, with Cy7-DOX-NPs (**11**) reaching 75% of the nanofection compared to 15% of the HP-Cy7-DOX-NPs (**14**). These results corroborate the nonspecific entry of NPs in absence of CRGDK.

Although the data reported so far could suggest a selective uptake of these theranostic NPs (HP-Cy7-DOX-NPs (**14**)) due to specific cell targeting, we also proceed with a deeper study that could provide more relevant information. Hence, the specificity of the cellular uptake was further investigated by competitive binding experiments with free CRGDK homing peptide. Cells were preincubated with CRDGK for 6 hours and afterwards treated with HP-Cy7-DOX-NPs (**14**) and Cy7-DOX-NPs (**11**) for 15 hours. Cell binding sites were effectively blocked by the free homing peptide, reducing significantly the uptake of the theranostic NPs (HP-Cy7-DOX-NPs (**14**)) (Figure 3, *E*). Furthermore, uptake levels of tested Cy7-DOX-NPs (**11**) remained consistent despite free homing peptide treatment. These data also support the specific and receptor-mediated binding mechanism of HP-Cy7-DOX-NPs (**14**) and its significantly enhanced targeting activity with Nrp-1 overexpressing cancer cells.

*Theranostic NPs increase in vitro therapeutic efficacy of doxorubicin in triple negative breast cancer cells*

The cytotoxic effect of DOX conjugated to theranostic NPs (HP-Cy7-DOX-NPs (**14**)) was evaluated by measuring the cell-mediated reduction of sodium resarzurin, a standard colorimetric and quantitative method that determines the cell viability on MDA-MB-231 cells.[28] Half maximal inhibitory concentration ($IC_{50}$) was determined and compared with cell incubation with free DOX. A range of different NPs concentrations were incubated for 96 hours with MDA-MB-231 cells. $IC_{50}$ value for theranostic NPs (HP-Cy7-DOX-NPs (**14**)) was calculated to be 41 nM (Figure 4, *A*), which correspond to 2250 NPs/cell (Figure S5, *B*). As previously reported, free DOX completely inhibited cell growth at 1000 nM, having an $IC_{50}$ of 120 nM in MDA MB 231 cells (Figure S5, *A*). These values indicated that DOX conjugated to the NPs reduced the $IC_{50}$ value with respect to free DOX. As result, this nanosytem offers a three-fold reduction of the amount of DOX required to have the same effect than free DOX in tumor cells. These finding demonstrate that HP-Cy7-DOX-NPs (**14**) could effectively target tumor cells overexpressing Nrp-1 receptors and subsequently enhance the tumor selective therapeutic effect of DOX.

Finally, the $IC_{90}$ of HP-Cy7-DOX-NPs (**14**) against MDA-MB-231 cells was determined. The value of $IC_{90}$ was 500 nM that correspond to 20,000 NPs/Cell. It was observed that the reduction of cell viability was enhanced by using HP-Cy7-DOX-NPs (**14**) when compared to free DOX (Figure 4, *B*). Cell viability was reduced from 26% to 15% by using NPs. It is important to remark that the Naked NPs (**1**) without DOX have not effect on the cell viability of the MDA MB 231 cell line (Figure 4, *B*).

*Theranostic NPs have in vivo targeted therapeutic efficiency against triple negative breast cancer avoiding side effects of doxorubicin and tracking treatment response in real time*

To investigate *in vivo* therapeutic and tracking efficiency of these theranostic NPs (HP-Cy7-DOX-NPs (**14**)), comparative efficacy studies were carried out. An orthotopic xenotransplant of the triple-negative human breast cancer cell line MDA-MB231 was performed in immunosuppressed female NSG mice. The mice (5 per group) were divided into 3 groups and treated in accordance with the protocol approved by the Institutional Committee for Animal Care and Use (IACUC) of the University

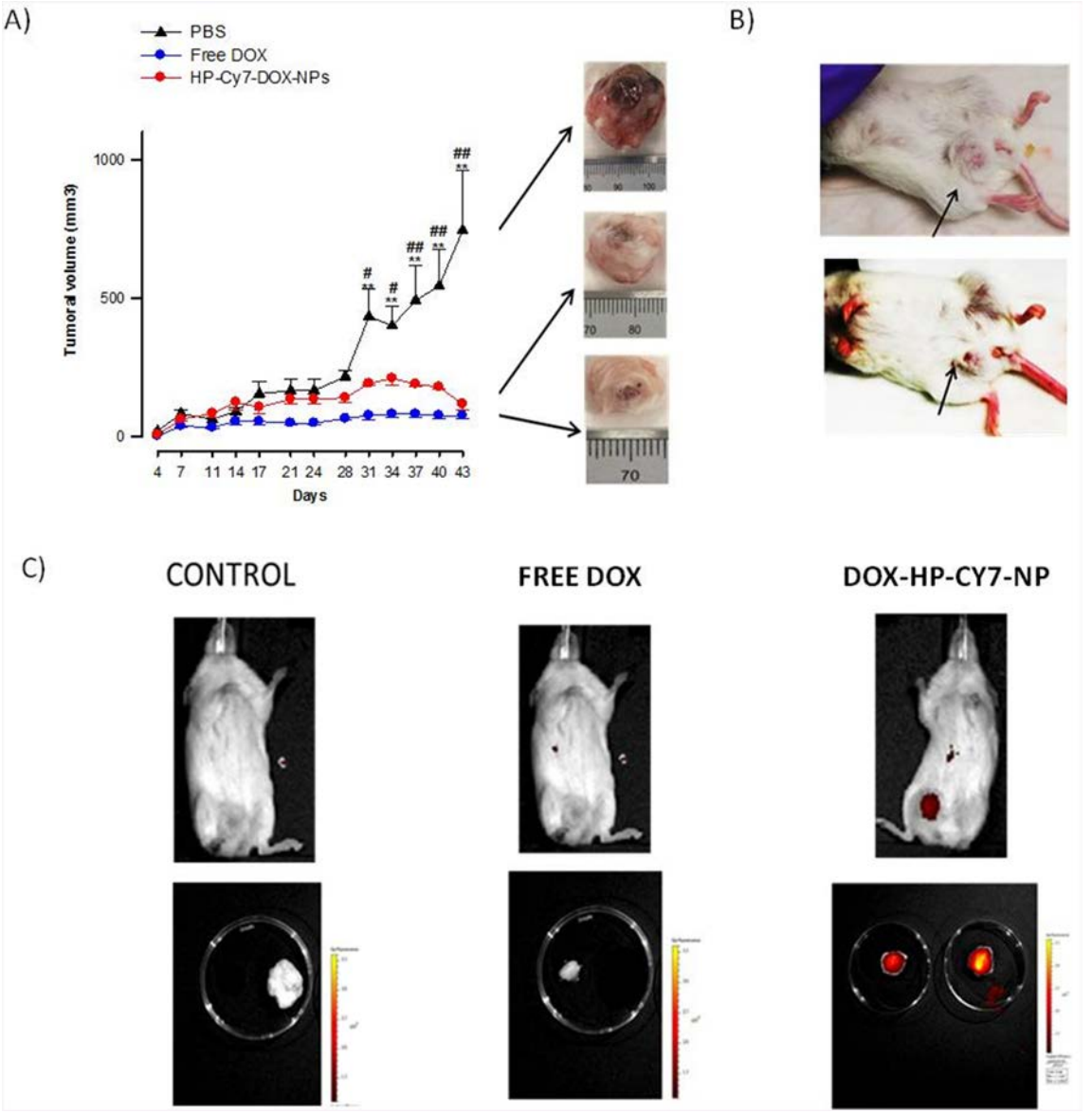


Figure 5. *In vivo* evaluation of therapeutic efficacy of intravenous administration of theranostic NPs (HP-Cy7-DOX-NPs (14)) in comparison with free DOX and PBS in NSG mice with tumors induced in the breast by inoculation of MDA-MB-231 cells in matrigel. A) Representation of relative change of tumor volume (mm3) over time of each group of mice during 43 days of treatment. Each point and vertical line represent the mean ± SEM (n = 5 per group). Statistically significant differences between PBS and free DOX treated groups $^{*}P \leq 0.05$; $^{**}P \leq 0.01$; and PBS *vs.* HP-Cy7-DOX-NPs $^{\#}P \leq 0.05$; $^{\#\#}P \leq 0.01$ on the same day after treatment (2-way repeated measures ANOVA followed by Bonferroni test). B) Images of orthotopic tumors in the breast of untreated mice (top image) and those treated with trifunctionalized NPs (bottom image) where a lower tumor volume is observed. C) *In vivo* fluorescence analysis (IVIS) of nanoparticle detection compared to negative controls in mice and isolated tumors.

of Granada and the Andalusian Regional Government in accordance with the European Directive for the protection of animals used for scientific purposes (2010/63/EU) and the Spanish law (Royal Decree 53/2013) (see SI). The treatment with PBS, free DOX and theranostic NPs (HP-Cy7-DOX-NPs (**14**)) was administered during 43 days, considering time zero when the tumor reached a size of 100 $mm^3$. Periodic intravenous administrations were done to each group of mice every 3 days. Figure 5 represents the changes in the relative tumor volume as a function of the treatment time. Mice treated with free DOX showed a significant tumor growth inhibition after 3 weeks. This therapeutic effect was evident for theranostic NPs after 28 days, where a decrease in tumor volume was observed arriving on day 43 to be similar to mice treated with free DOX (Figure 5, *A* and *B*). These results show that HP-Cy7-DOX-NPs (**14**) have a clear therapeutic effect similar to that of free DOX. Remarkably, fluorescence intensity analysis by IVIS showed that the trifunctionalized NPs (HP-Cy7-DOX-NPs (**14**)) were effectively tracked *in vivo* thanks to the conjugation of the fluorophore onto the nanoparticle and selectively accumulated in the mammary tumor mass and not in the rest of organs thanks to the functionalization with the CRGDK homing peptide (Figure 5, *C*).

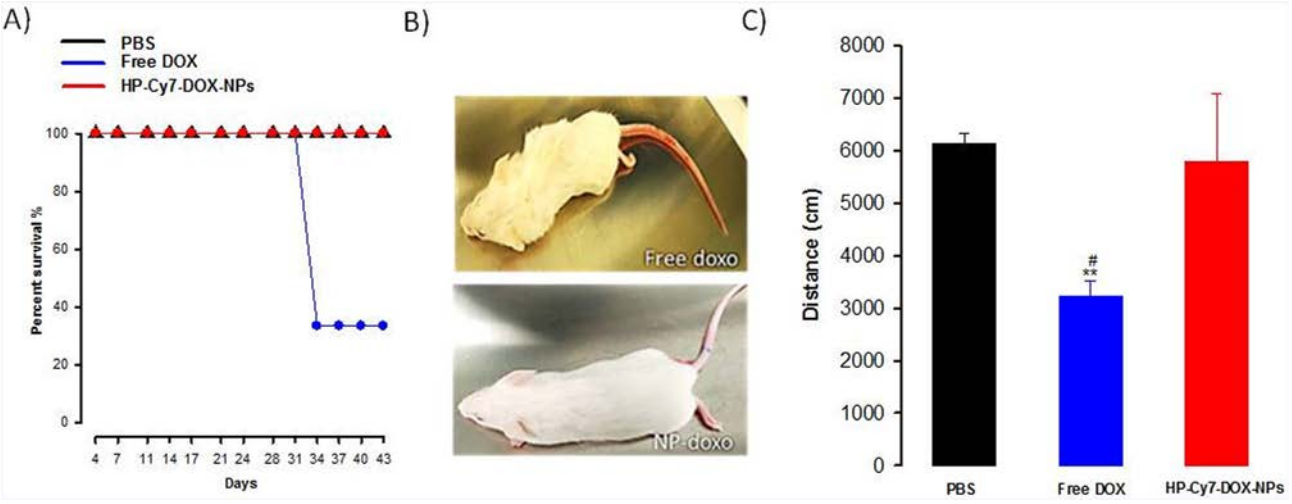


Figure 6. Evaluation of the toxicity of the theranostic nanosystem. A) Kaplan–Meier survival curve B) Comparative study of external signs of toxicity in mice treated with free DOX and theranostic NPs. C) Analysis of weight variation during treatment. Each point and vertical line represent the mean ± SEM (n = 5 per group). D) Analysis of activity based on the movement capacity (24 hours) of the treated mice *versus* control mice without treatment. Statistically significant differences between PBS and free DOX treated groups $^{**}P \leq 0.01$; and HP-Cy7-DOX-NPs *vs.* Free DOX $^{\#}P \leq 0.05$ (2-way repeated measures ANOVA followed by Bonferroni test).

Histological analysis of orthotopic xenograft tumor tissues further confirmed the therapeutic efficacy of HP-Cy7-DOX-NPs (**14**). As shown in Figure S6, xenograft tumors of the control group were composed of tightly packed and proliferative tumor cells (Figure S6, *A*). However, in xenograft tumors from treatment groups, the cellularity was significantly decreased, with typical apoptotic features such as small nuclear fragments surrounded by a rim of clear cytoplasm were observed more frequently in theranostic NPs-treated than DOX-treated tumors (Figure S6, *B* and *C*).

These *in vivo* findings demonstrate the efficient targeted delivery and enhanced therapeutic activity of these theranostic NPs in Nrp-1 overexpressing triple negative breast cancer tumors. Previously, CRGDK peptide-functionalized nanomedicines were also reported to afford good targetability to MDA-MB-231 cells *in vitro* and *in vivo*.[29,30]

Additionally, a series of experiments were carried out to monitor the *in vivo* toxicity of the treatment. First, a comparative analysis of the survival of mice treated with the theranostic nanoparticles (HP-Cy7-DOX-NPs (**14**)) *versus* mice treated with free DOX and untreated control mice (PBS) was carried out during the treatment period (43 days). In Figure 6, *A* it can be observed as the percentage of survival during the treatment period was 100% for both the mice treated with NPs and those that control group. However, treatment with DOX caused a high impact on survival. After 30 days of treatment there was a drastic decrease in the percentage of survival (30%). This effect could be attributed to the inherent systemic toxicity of this antitumor drug[31] and to the serious side effects of this conventional chemotherapy treatment. Indeed, an analysis of the physical appearance of the treated mice corroborates this result. Figure 6, *B* shows a representative image of a mouse treated with free DOX where evident external signs of toxicity are observed in comparison with a mouse form the group treated with theranostic nanoparticles (HP-Cy7-DOX-NPs (**14**)). The main external side effects observed in mice treated with free DOX were weight loss, piloerection, behavior disorders and damaged tail, among others. The most striking side effect was the high cutaneous toxicity produced in the tail of the mice treated with DOX (Figure 6, *B*, top image). Also, a significant weight reduction was found in mice treated with free DOX in comparison to weight in both control untreated or theranostic NPs-treated mice (Figure 6, *C*). Additionally, to observe the toxic effect of the treatment at the level of the central nervous system, a standardized protocol to test movement was carried out at day 30 in a cage with a camera prepared for this purpose. This camera analyzes the distance traveled by the mouse during 24 hours. Treatment with HP-Cy7-DOX-NPs (**14**) did not affect the motor activity being comparable to that of the untreated mice; however, free DOX caused a significant decrease of mice mobility (Figure 6, *C*). In metastatic breast cancer, DOX treatment has several adverse effects including cardiotoxicity, skin and hematological toxicities due to lack of selectivity, which subsequent provoke the therapeutic failure.[32] .Our results suggest that DOX loaded to theranostic NPs significantly avoids important side effects.

## Discussion

In this study, we reported for the first time a successfully developed theranostic nanodevice based on orthogonal conjugation strategies for the multifunctionalization of polymeric NPs. Theranostic NPs (HP-Cy7-DOX-NPs (**14**)) containing controlled amount of each one of the components has been successfully prepared. A selective receptor-mediated release of DOX has been successfully achieved in TNBC cells overexpressing Nrp-1 by CRGDK peptide conjugation.

We used an orthogonal strategy to achieve the efficient covalent tri-functionalization of NPs. This included PEGylation to increase the half-life of the circulating NPs and to reduce the unfavorable interactions between the different molecules

conjugated to the NPs, but also to evade opsonization and subsequent phagocytosis.[23] Moreover, DOX was bound to the NPs through a pH labile hydrazone bond to allow the release of DOX *via* the pH sensitive hydrazine linker in a sustained manner in both tumor cells (lysosomes: pH 4–5, endosomes: pH 5–6) and tumor microenvironments (pH 6.5–7.2), which present lower pH values due to hypoxia if compared with that in bloodstream (pH 7.4).[33] The sustained drug release of HP-Cy7-DOX-NPs (**14**) up to 168 h at pH 5.2 suggests that in acidic tissues such as tumoral tissues could be a very beneficial feature to prolong and improve the therapeutic efficacy of NPs and validates the drug release strategy selected for this study.

In addition, CRGDK (Cys-Arg-Gly-Aps-Lys) homing peptide was coupled the NPs *via* chemoselective conjugation to target TNBC cells overexpressing Nrp-1. This transmembrane receptor glycoprotein is involved in nervous system development and angiogenesis and, also, is overexpressed on the surface of a wide variety of tumors and it has a crucial role in TNBC tumorigenesis and metastasis. Nrp-1 is a useful targeting site for tumor-specific drug delivery and selective anti breast cancer strategies.[34] In fact, CRGDK-mediated targeting has been widely demonstrated to be able to increase the affinity for tumor cells and facilitate the drug-loaded NPs to efficiently enter the cells through ligand-receptor mediated endocytosis.[35–37] Our *in vitro* results showed the nonspecific entry of NPs in absence of the homing peptide and after the selective blockage of receptor, supporting the specific and receptor-mediated binding mechanism of HP-Cy7-DOX-NPs (**14**) and its significantly enhanced targeting activity with Nrp-1 overexpressing cancer cells. Moreover, cytotoxicity assays showed three-fold reduction of the amount of DOX required to have the same effect than soluble DOX in MDA-MB-231 cells, which indicate the ability of our targeted theranostic nanosystem to increase the antitumor potency of DOX.

In agreement with these results, CRGDK peptide-functionalized nanomedicines were also reported to afford good targetability to MDA-MB-231 TNBC cells *in vitro* and *in vivo*.[29,30] Nowadays, several reports have demonstrated that attaching this peptide to different types of NPs, they are capable of specifically recognize the Nrp-1 receptor and increase the *in vivo* cytotoxic effect of vehiculized drugs.[35,38–40]

To investigate the *in vivo* therapeutic and tracking efficiency of these theranostic NPs (HP-Cy7- DOX-NPs (14)), comparative efficacy studies were carried out. An orthotopic xenotransplant of the MDA-MB231 TNBC cell line was performed in immunosuppressed female NSG mice while not appreciable side effects were observed. These *in vivo* experiments demonstrate the efficient targeted delivery and enhanced therapeutic activity of these theranostic NPs in Nrp-1 overexpressing TNBC tumors. Remarkably, *in vivo* fluorescence tracking analysis showed the preferable location of theranostic NPs in the tumor area reducing the volume in a similar grade than free DOX. The choice of a near infrared tracker (Cy7 fluorophore) allowed and efficient monitoring by fluorescence analysis with low background and high signal-to-noise ratio. These properties make near infrared fluorescent dyes of great interest for bioimaging applications.[41] A comparative analysis of the survival of mice treated with the theranostic nanoparticles (HP-Cy7-DOX-NPs (14)) *versus* mice treated with free DOX and untreated control mice (PBS) was carried out during the treatment period, showing lower survival rates for free DOX (30%) than those treated with theranostic NPs (100%). The effect of free DOX could be attributed to the inherent systemic toxicity of this antitumor drug[31] and to the serious side effects of this conventional chemotherapy treatment. Indeed, an analysis of the physical appearance of the treated mice corroborates this result. In metastatic breast cancer, DOX treatment has several adverse effects including cardiotoxicity, skin and hematological toxicities due to lack of selectivity, which subsequent provoke the therapeutic failure.[32] Our results suggest that DOX loaded to theranostic NPs significantly avoids important side effects.

In summary, we reported for the first time a successfully developed theranostic nanodevice based on orthogonal conjugation strategies for the multifunctionalization of polymeric NPs. Theranostic NPs (HP-Cy7-DOX-NPs (**14**)) containing controlled amount of each one of the components has been successfully prepared. Remarkably, near infrared fluorescent labeling (Cy7 tracker) allows efficient *in vivo* tracking of the nanodevice. In addition, this mutifunctionalized theranostic platform is a potent candidate for the treatment of Nrp-1 overexpressing tumors and it is also a good system to avoid the adverse effects associated with traditional chemotherapy.

It is important to note that several modifications can be made in this novel nanosystem that broaden the range of applications of this prototype such as binding of different drugs, alternative use of other tracker molecules depending on the detection technique used and conjugation of other specific peptide sequences for different tumors and even for different pathological areas. In the near future, further studies will be carried out to evaluate the versatility of this theranostic nanodevice.

## Appendix A. Supplementary data

Supplementary data to this article can be found online at https://doi.org/10.1016/j.nano.2019.102120.

## References

1. Elsabahy M, Heo GS, Lim S-M, Sun G, Wooley KL. Polymeric nanostructures for imaging and therapy. *Chem Rev* 2015;**115**:10967-1011.
2. Lim E-K, Kim T, Paik S, Haam S, Huh Y-M, Lee K. Nanomaterials for theranostics: recent advances and future challenges. *Chem Rev* 2015;**115**:327-94.
3. Ang CY, Tan SY, Teh C, Lee JM, Wong MFE, Qu Q, et al. Redox and pH dual responsive polymer based nanoparticles for in vivo drug delivery. *Small* 2017;**13**1602379.
4. Ponzoni M, Curnis F, Brignole C, Bruno S, Guarnieri D, Sitia L, et al. Enhancement of tumor homing by chemotherapy-loaded nanoparticles. *Small* 2018;**14**1802886.
5. Unciti-Broceta A, Díaz-Mochón JJ, Sánchez-Martín RM, Bradley M. The use of solid supports to generate nucleic acid carriers. *Acc Chem Res* 2012;**45**:1140-52.
6. Cardenas-Maestre JM, Panadero-Fajardo S, Perez-Lopez AM, Sanchez-Martin RM. Sulfhydryl reactive microspheres for the efficient delivery of thiolated bioactive cargoes. *J Mater Chem* 2011;**21**:12735-43.

7. Loos C, Syrovets T, Musyanovych A, Mailänder V, Landfester K, Nienhaus GU, et al. Polystyrene nanoparticles as a platform for studying nano interactions. *Beilstein J Nanotechnol* 2014;**5**:2403-12.
8. Borger JG, Cardenas-Maestre JM, Zamoyska R, Sanchez-Martin RM. Novel strategy for microsphere-mediated DNA transfection. *Bioconjug Chem* 2011;**22**:1904-8.
9. Yusop RM, Unciti-Broceta A, Johansson EMV, Sánchez-Martín RM, Bradley M. Palladium-mediated intracellular chemistry. *Nat Chem* 2011;**3**:239-43.
10. Tsakiridis A, Alexander LM, Gennet N, Sanchez-Martin RM, Livigni A, Li M, et al. Microsphere-based tracing and molecular delivery in embryonic stem cells. *Biomaterials* 2009;**30**:5853-61.
11. Alexander LM, Pernagallo S, Livigni A, Sánchez-Martín RM, Brickman JM, Bradley M. Investigation of microsphere-mediated cellular delivery by chemical, microscopic and gene expression analysis. *Mol Biosyst* 2010;**6**:399-409.
12. Cárdenas-Maestre JM, Pérez-López AM, Bradley M, Sánchez-Martín RM. Microsphere-based intracellular sensing of Caspase-3/7 in apoptotic living cells. *Macromol Biosci* 2014;**14**:923-8.
13. Patricia Altea-Manzano, Juan Diego Unciti-Broceta, Victoria Cano-Cortes, María Paz Ruiz-Blas, Teresa Valero-Griñan, Juan Jose Diaz-Mochon, R.S.-M. Tracking cell proliferation using a nanotechnology-based approach. *Nanomedicine* 2017;**12**:1591-605.
14. Valero T, Delgado-González A, Unciti-Broceta JD, Cano-Cortés V, Pérez-López AM, Unciti-Broceta A, et al. Drug "clicking" on cell-penetrating fluorescent nanoparticles for *In Cellulo* chemical proteomics. *Bioconjug Chem* 2018;**29**:3154-60.
15. Naik A, Al-Zeheimi N, Bakheit CS, Al Riyami M, Al Jarrah A, Al Moundhri MS, et al. associated molecules in the blood distinguish poor prognosis breast Cancer: a cross-sectional study. *Sci Rep* 2017;**7**:3301.
16. Unciti-Broceta A, Johansson E, Yusop Rahimi M, Sánchez-Martín RM, Bradley M. Synthesis of polystyrene microspheres and functionalization with Pd0 nanoparticles to perform bioorthogonal organometallic chemistry in living cells. *Nat Protoc* 2012;**7**:1207-18.
17. Picon-Ruiz M, Pan C, Drews-Elger K, Jang K, Besser AH, Zhao D, et al. Interactions between adipocytes and breast Cancer cells stimulate cytokine production and drive Src/Sox2/miR-302b–mediated malignant progression. *Cancer Res* 2016;**76**:491-504.
18. Unciti-Broceta JD, Cano-Cortés V, Altea-Manzano P, Pernagallo S, Díaz-Mochón JJ, Sánchez-Martín RM. Number of nanoparticles per cell through a spectrophotometric method - a key parameter to assess nanoparticle-based cellular assays. *Sci Rep* 2015;**5**:1-10.
19. Kaiser E, Colescott RL, Bossinger CD, Cook PI. Color test for detection of free terminal amino groups in the solid-phase synthesis of peptides. *Anal Biochem* 1970;**34**:595-8.
20. Fields GB, Noble RL. Solid phase peptide synthesis utilizing 9-fluorenylmethoxycarbonyl amino acids. *Int J Pept Protein Res* 1990;**35**:161-214.
21. Díaz-Mochón JJ, Bialy L, Bradley M. Full orthogonality between Dde and Fmoc: the direct synthesis of PNA-peptide conjugates. *Org Lett* 2004;**6**:1127-9.
22. Bycroft, B.W.; Chan, W.C.; Chhabra, S.R.; Hone, N.D. A novel lysine-protecting procedure for continuous flow solid phase synthesis of branched peptides. J Chem Soc Chem Commun 1993, ***0***, 778.
23. Yang K, Ma Y-Q. Computer simulation of the translocation of nanoparticles with different shapes across a lipid bilayer. *Nat Nanotechnol* 2010;**5**:579-83.
24. Thielbeer F, Johansson EMV, Chankeshwara SV, Bradley M. Influence of spacer length on the cellular uptake of polymeric nanoparticles. *Macromol Biosci* 2013;**13**:682-6.
25. Wiechelman KJ, Braun RD, Fitzpatrick JD. Investigation of the bicinchoninic acid protein assay: identification of the groups responsible for color formation. *Anal Biochem* 1988;**175**:231-7.
26. Taherian A, Li X, Liu Y, Haas TA. Differences in integrin expression and signaling within human breast cancer cells. *BMC Cancer* 2011;**11**:293.
27. Chalakur-Ramireddy NKR, Pakala SB. Combined drug therapeutic strategies for the effective treatment of triple negative breast Cancer. *Biosci Rep* 2018;**38**.
28. O'Brien J, Wilson I, Orton T, Pognan F. Investigation of the Alamar blue (resazurin) fluorescent dye for the assessment of mammalian cell cytotoxicity. *Eur J Biochem* 2000;**267**:5421-6.
29. Liu P, Qin L, Wang Q, Sun Y, Zhu M, Shen M, et al. cRGD-functionalized mPEG-PLGA-PLL nanoparticles for imaging and therapy of breast cancer. *Biomaterials* 2012;**33**:6739-47.
30. Jin G, Feng G, Qin W, Tang BZ, Liu B, Li K Multifunctional organic nanoparticles with aggregation-induced emission. (AIE) characteristics for targeted photodynamic therapy and RNA interference therapy. *Chem Commun (Camb)* 2016;**52**:2752-5.
31. Minotti G, Menna P, Salvatorelli E, Cairo G, Gianni L. Anthracyclines: molecular advances and pharmacologic developments in antitumor activity and cardiotoxicity. *Pharmacol Rev* 2004;**56**:185-229.
32. Shafei A, El-Bakly W, Sobhy A, Wagdy O, Reda A, Aboelenin O, et al. A review on the efficacy and toxicity of different doxorubicin nanoparticles for targeted therapy in metastatic breast cancer. *Biomed Pharmacother* 2017;**95**:1209-18.
33. No Manchun S, Dass CR, Sriamornsak P. Targeted therapy for cancer using Ph-responsive nanocarrier systems. *Life Sci* 2012;**90**:381-7.
34. Arpel A, Gamper C, Spenlé C, Fernandez A, Jacob L, Baumlin N, et al. Inhibition of primary breast tumor growth and metastasis using a neuropilin-1 transmembrane domain interfering peptide. *Oncotarget* 2016;**7**:54723-32.
35. Kumar A, Huo S, Zhang X, Liu J, Tan A, Li S, et al. Neuropilin-1-targeted gold nanoparticles enhance therapeutic efficacy of platinum(IV) drug for prostate Cancer treatment. *ACS Nano* 2014;**8**:4205-20.
36. Fan X, Zhang W, Hu Z, Li Z. Facile synthesis of RGD-conjugated unimolecular micelles based on a polyester dendrimer for targeting drug delivery. *J Mater Chem B* 2017;**5**:1062-72.
37. Yang M, Yu L, Guo R, Dong A, Lin C, Zhang J. A modular coassembly approach to all-in-one multifunctional Nanoplatform for synergistic codelivery of doxorubicin and curcumin. *Nanomaterials* 2018;**8**:167.
38. Liu X, Si J, Zhang Q, Huang Q, Gu D, Yang H, et al. Functionalized nanoparticles efficiently enhancing the targeted delivery, tumor penetration, and anticancer activity of 7-Ethyl-10-Hydroxycamptothecin. *Adv Healthc Mater* 2018;**7**.
39. Liu H, Shi X, Wu D, Kahsay Khshen F, Deng L, Dong A, et al. Injectable, biodegradable, Thermosensitive nanoparticles-aggregated hydrogel with tumor-specific targeting, penetration, and release for efficient postsurgical prevention of tumor recurrence. *ACS Appl Mater Interfaces* 2019;**11**:19700-11.
40. Wei T, Liu J, Ma H, Cheng Q, Huang Y, Zhao J, et al. Functionalized nanoscale micelles improve drug delivery for cancer therapy in vitro and in vivo. *Nano Lett* 2013;**13**:2528-34.
41. Escobedo JO, Rusin O, Lim S, Strongin RM. NIR dyes for bioimaging applications. *Curr Opin Chem Biol* 2010;**14**:64-70.